Research Article | Vol. 27, No. 23 / 11 November 2019 / Optics Express 34079
Optics EXPRESS

Ground-to-air FSO communications: when high data rate communication meets efficient energy harvesting with simple designs

CHADI ABOU-RJEILY,[1,4] GEORGES KADDOUM,[2,5] AND GEORGE K. KARAGIANNIDIS[3,6]

[1]Department of Electrical and Computer Engineering, Lebanese American University (LAU), Byblos, Lebanon
[2]LACIME Laboratory, University of Québec, ÉTS Engineering School, Montreal, Canada
[3]Department of Electrical and Computer Engineering, Aristotle University of Thessaloniki, Thessaloniki, Greece
[4]chadi.abourjeily@lau.edu.lb
[5]georges.kaddoum@etsmtl.ca
[6]geokarag@auth.gr

Abstract: The capability of free-space optical (FSO) communications in delivering very high data rates and the agility of unmanned aerial vehicle (UAV) flying platforms render FSO-UAV-based solutions attractive for delivering 5G wireless communication services. In parallel, research on simultaneous information and power transfer, whether in the context of radio frequency (RF) networks or indoor optical wireless communication (OWC) networks, is on the rise. Even though the operation of a UAV is limited by its battery lifetime, the concept of energy harvesting (EH) from the information-carrying FSO signals was not deeply investigated in the literature. This paper highlights the inherent EH capabilities in FSO transmissions and investigates novel signal design methodologies for boosting the EH efficiency. We focus on the ground-to-air communications where the ground-based FSO transmitter is connected to the power grid and, hence, is governed by a peak-power constraint and not an average-power constraint. For this setup, simulations carried out under different weather conditions demonstrate that high data rates can be associated with significant amounts of harvested energy using simple transceiver architectures.

1. Introduction, background and contribution

1.1. Introduction

Optical wireless communication (OWC) constitutes a key technology for 5G wireless networks. OWC alleviates the radio frequency (RF) spectrum crunch problem by enabling communications in the visible, infrared and ultraviolet optical frequency bands for a variety of indoor and outdoor applications. Outdoor infrared OWC systems are widely referred to as free-space optical (FSO) communications that rely on line-of-sight transmissions of narrow laser beams. The FSO technology is license-free, easy-to-deploy, cost-effective and capable of delivering very high data rates [1]. On the other hand, the usage of drones, also known as unmanned aerial vehicles (UAVs), has attracted increasing attention recently due to the agility and scalability of the networked flying platforms (NFPs). UAVs have been widely used in the military and commercial domains [2]. Commercial applications include downlink transmissions, remote sensing, monitoring, search and rescue, and security [3]. The deployment of UAVs is expected to rise at unprecedented rates due to growing interest from investors, researchers and hobbyists [4].

Driven by the benefits of FSO communications and UAV platforms, recent studies investigated merging these two key technologies for a variety of practical applications [5,6]. In [5], FSO-UAV-based solutions were proposed to provide efficient backhauling/fronthauling to small cell base

#367718 https://doi.org/10.1364/OE.27.034079
Journal © 2019 Received 15 May 2019; revised 17 Oct 2019; accepted 27 Oct 2019; published 7 Nov 2019

Optics EXPRESS

stations (SBSs). In this context, UAVs transport the data traffic between the SBSs and the core network through highly directive FSO links. The proposed FSO-UAV framework complements the terrestrial wireless and wired solutions while delivering very high data rates. The integration of the FSO and UAV technologies was also considered in [6] in the context of relay-assisted communications. Following from the vulnerability of the FSO links to the underlying weather conditions, quasi-stationary and moving buffer-aided UAVs can boost the reliability of the optical wireless network by adapting their hovering positions to the states of the source-destination, source-relay and relay-destination FSO channels.

In order to further capitalize on the benefits that can be reaped from the FSO-UAV platforms, this paper explores the additional degree of freedom pertaining to energy harvesting (EH) at such platforms. In particular, we focus on the free energy that can be harvested from the information-carrying signals communicated from terrestrial FSO stations. This scenario is particularly appealing since the terrestrial FSO stations are connected to the electric power grid. Consequently, the average amount of transmitted power is not problematic at these stations compared to UAVs or other battery-powered devices. Figure 1 provides an illustration of a FSO-UAV-based framework with EH from the ground FSO stations.

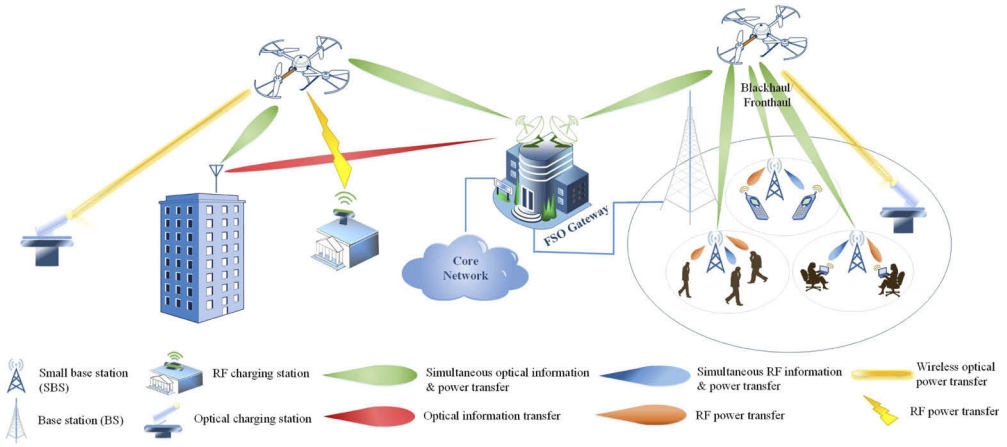

Fig. 1. Graphical illustration of FSO-UAV-based relay-assisted and backhaul/fronthaul frameworks for 5G wireless networks.

1.2. Background

In the era of 5G communications, EH techniques are of fundamental importance for prolonging the network lifetime. EH at the mobile nodes can be achieved through wireless power transfer (WPT) from dedicated and fully controlled power sources like base stations. Examples of far-field RF WPT include [7] where the RF energy is transferred from UAVs to mobile nodes deployed in ultra dense networks (UDNs). Besides the RF WPT techniques, EH through optical WPT is on the rise. For example, laser beam power transfer was considered in [8] where a ground-based laser delivers optical energy to charge a UAV in flight. A similar application was outlined in [9] in the scenario where a FSO transmitter with permanent power supply communicates with a receiver with no power supply. In this case, the packet duration is slotted and the energy harvested in the first slot is used to convey the information during the second slot.

Putting in place dedicated sources to solely provide RF or optical WPT incurs additional network deployment costs. Moreover, this deployment increases the exposure of people and living things to dangerous power laser beams and excessive electromagnetic radiation in uncontrolled environments. These drawbacks of WPT motivated the investigation of a new paradigm to integrate

Optics EXPRESS

information transmission and power transfer through the simultaneous wireless information and power transfer (SWIPT) concept introduced in [10]. Among the numerous applications of RF SWIPT, [11] proposed to concurrently transfer information and power from base stations (BSs) to UAVs and from UAVs to mobile nodes. The tradeoff between the information rate and harvested energy level arises as a major design parameter in SWIPT systems.

While the RF SWIPT technology has been well investigated in the last ten years, simultaneous lightwave information and power transfer (SLIPT) emerged recently [12,13]. The SLIPT technology was investigated in the context of indoor OWC systems where the visible (and potentially infrared) light emitted by the light emitting diodes (LEDs) transports information and optical power to the mobile users [12]. This technology was also considered in [13] in the context of outdoor ground-to-air (GtA) FSO communications. The SLIPT concept revolves around solar panel based receivers where the direct current (DC) and alternating current (AC) components of the received optical signal are separated and used for EH and information decoding (ID), respectively [12,13].

The SLIPT solutions revolve around time-splitting (TS) and average power (AP) optimization [12,13]. They include:

- SLIPT-TS: the transmission time is slotted into two slots. Over the first slot, the AP value is fixed at the center of the laser's linear operating region. Over the second slot, the optical source transmits at peak power (PP) in an attempt to improve the EH. This solution was considered in [13] for GtA FSO communications.

- SLIPT-TS-AP: over the first slot, the AP value is optimized and, over the second slot, the source transmits at PP.

While the SLIPT-TS-AP protocol results in improved levels of EH compared to SLIPT-TS, the former strategy is more complicated than the latter one. In fact, SLIPT-TS-AP involves the optimization of two variables (TS ratio and AP) while SLIPT-TS requires solving for the TS ratio only.

1.3. Contributions

The battery lifetime is of predominant importance in NFPs usually entailing stringent weight constraints and power consumption limitations. Consequently, a major challenge in conceiving EH solutions for UAVs resides in controlling the additional EH-related processing overhead that increases the power consumption. In particular, overhead, in the form of algorithmic optimization, channel state information (CSI) and heavy information exchange over feedback channels, must be kept at a minimum; otherwise, the amount of harvested energy might be compromised by the energy expended to implement the EH solution.

The aforementioned challenge is pivotal to this work that targets the design of EH-efficient FSO schemes that can be implemented at the UAVs in a simple manner. This target is achieved by taking the specificities of the FSO communications into consideration for advising novel EH schemes that are adapted to the pulse-based modulations often associated with FSO; namely, pulse amplitude modulation (PAM) and pulse position modulation (PPM). This modulation-specific EH design approach clearly distinguishes this work from the existing OWC EH schemes.

The contributions of this paper are threefold:

- This work proposes a novel way for realizing EH with PAM signalling under a fixed PP constraint. This approach is compared with the SLIPT-TS-AP and SLIPT-TS solutions [12] under different weather conditions. Results show that the proposed scheme achieves the same EH levels as SLIPT-TS-AP while involving the optimization over only one parameter in a manner that is analogous to SLIPT-TS. We also show that the involved optimization can be implemented in a simple manner, hence, meeting the EH design complexity constraints at the UAVs.

Optics EXPRESS

- Unlike SLIPT solutions that are not tied to a selected modulation format, we advise novel EH PPM techniques that are adapted to the specificities of the PPM constellations. One of the proposed EH methods can be implemented in a seamless manner without the need of carrying out any optimization while precluding all forms of CSI acquisition. These distinctive features differentiate the PPM-specific method from the SLIPT techniques.
- The article recommends an innovative EH-efficient modulation scheme for FSO IM/DD communications. The suggested scheme benefits from the same advantages of PPM while supplying higher levels of EH.

The proposed schemes allow to achieve different levels of tradeoff between EH-efficiency and complexity. Since EH is not required in ground-to-ground (GtG) and air-to-air (AtA) applications, the key attributes of this work are most suitable for GtA FSO-UAV frameworks.

2. System model

2.1. FSO communications

2.1.1. Modulation formats

Non-coherent FSO solutions based on intensity-modulation and direct-detection (IM/DD) constitute the most popular form of FSO communication systems. This non-coherent communication format is remarkably simple compared to coherent FSO systems based on superheterodyne detection [1]. This remarked simplicity renders the FSO IM/DD approach the most suitable option for UAV platforms that have limited processing capabilities and that are subject to stringent weight and power-consumption constraints. In order to maintain a linear relationship between the transmitted optical power and driving electrical current, the modulation of the laser must be limited to its linear operating region. Optical powers in this region surpass the lasing threshold while not exceeding the PP above which nonlinear effects are manifested. In this context, the average power transmitted by the laser will be denoted by P_{av} where:

$$P_{\min} \leq P_{\text{av}} \leq P_{\max}, \tag{1}$$

where $P_{\min}$ and $P_{\max}$ denote the threshold power and PP, respectively.

FSO IM/DD communications are most commonly associated with either pulse amplitude modulation (PAM) or pulse position modulation (PPM). For PAM, the information is encoded in the levels of the transmitted optical power where Q power levels are selected in the linear region $[P_{\min} \;\; P_{\max}]$ for the purpose of realizing Q-ary modulation. The unipolar PAM constellation is defined by selecting the Q power levels $\{P_q\}_{q=1}^{Q}$ such that:

$$P_{\min} \leq P_1 < \cdots < P_Q \leq P_{\max}. \tag{2}$$

In this work, we assume that the receiver is corrupted by additive white Gaussian noise (AWGN). This noise model constitutes a valid approximation in the case of background noise limited receivers where the shot noise caused by background radiation is dominant with respect to the other noise components such as thermal noise and dark currents [14]. In this scenario, the Q power levels are selected to be uniformly distributed in $[P_{\min} \;\; P_{\max}]$:

$$P_q = P_{\min} + \frac{q-1}{Q-1}\left[P_{\max} - P_{\min}\right] \;\; ; \;\; q = 1, \ldots, Q, \tag{3}$$

where this selection minimizes the bit error rate (BER) at the receiver under the AWGN assumption. Following from (3), the AP of the PAM constellation takes the following value:

$$P_{\text{av}}^{(\text{PAM})} = \frac{P_{\min} + P_{\max}}{2}. \tag{4}$$

Optics EXPRESS

The most common form of PAM is on-off-keying (OOK) where the laser is pulsed at minimum power $P_1 = P_{\min}$ for the transmission of a binary 0 and at maximum power $P_2 = P_{\max}$ for the transmission of a binary 1.

On the other hand, PPM constitutes an appealing easy-to-deploy alternative to PAM. For Q-PPM, the symbol duration is divided into Q slots with the laser pulsed at PP in only one of these slots. This results in the following AP value:

$$P_{\text{av}}^{(\text{PPM})} = \frac{1}{Q} P_{\max}, \tag{5}$$

since the Q-PPM symbol comprises only one "*on*" slot among the Q available slots.

While PAM signalling requires adapting the threshold detection levels to the channel turbulence conditions for the sake of attaining optimal performance, the optimal decodability of PPM does not require the acquisition of any type of channel state information (CSI). On the other hand, PAM signalling is more spectrally-efficient compared to unipolar PPM signalling.

2.1.2. FSO channel

The atmospheric weather conditions constitute the major impairment that limits the performance along outdoor optical links. The FSO signal is vulnerable to atmospheric attenuation, caused by absorption, scattering and turbulence, as well as other losses such as pointing losses [5,6,12]. Taking the above losses into consideration, the minimum, average and maximum optical powers that fall on the receiver can be written as: $\mathcal{P}_{\min} = 10^{-\frac{L_{\text{atm}}}{10}} P_{\min}$, $\mathcal{P}_{\text{av}} = 10^{-\frac{L_{\text{atm}}}{10}} P_{\text{av}}$ and $\mathcal{P}_{\max} = 10^{-\frac{L_{\text{atm}}}{10}} P_{\max}$, respectively. L_{atm} encompasses the atmospheric losses (in dB) and can be written as:

$$L_{\text{atm}} = \alpha h + L_{\text{tur}} + L_{\text{poi}} + L_{\text{rain}}, \tag{6}$$

where h stands for the altitude of the UAV and α stands for the attenuation coefficient (in dB/m). In (6), L_{tur}, L_{poi} and L_{rain} stand for the turbulence, pointing and rain losses, respectively. The pointing losses arise from the misalignment of the spot radius of the emitted light beam. These losses depend on a number of factors including the speed of the UAV, the link distance as well as the tracking system between the ground and aerial units. Emerging FSO systems implement tracking systems that are suitable to fast moving flying platforms in order to reduce the pointing losses [5].

In (6), the attenuation that results from the atmospheric turbulence, or scintillation, is related to the height h by the relation [5]:

$$L_{\text{tur}} = 2\sqrt{23.17 C_n^2 \left(\frac{2\pi}{\lambda} 10^9\right)^{\frac{7}{6}} h^{\frac{11}{6}}}, \tag{7}$$

where λ is the wavelength and C_n^2 is the refractive-index structure parameter that captures the scintillation severity. Scintillation results from the variations of the index of refraction due to inhomogeneities in temperature and pressure changes and it constitutes a major impairment that severely degrades the performance. The parameter C_n^2 depends on the underlying weather conditions as highlighted in Table 2.

2.2. EH model

In OWC, a DC bias is added to the information-carrying AC component in order to limit the modulation to the linear output-versus-input region of the optical source. For such operating scenario, the harvested energy increases with the DC value of the received signal or, equivalently,

Optics EXPRESS

with the AP transmitted by the optical source. In particular, the harvested energy is given by [12]:

$$E(P_{\text{av}}) = fV_t I_{\text{DC}} \ln\left(1 + \frac{I_{\text{DC}}}{I_0}\right), \tag{8}$$

where f, V_t and I_0 stand for the photo-detector's fill factor, thermal voltage and dark saturation current, respectively. In (8), I_{DC} stands for the DC component of the output current:

$$I_{\text{DC}} = \eta \mathcal{P}_{\text{av}} = \eta 10^{-\frac{L_{\text{atm}}}{10}} P_{\text{av}}, \tag{9}$$

where η stands for the receiver's responsivity (in A/W).

3. FSO-EH schemes

The following triad must be contemplated in the design of SLIPT-based systems; namely, the Quality-of-Service (QoS), the amount of harvested energy and the system complexity. The QoS level will be captured by the achievable information rate (in bits/second) that cannot exceed the channel capacity for an arbitrarily small probability of error. On the other hand, the system complexity is directly related to the level of CSI to be acquired and to the parameter optimization that needs to be carried out as will be further discussed at a later stage.

While the aforementioned design parameters constitute the bottom line for all IM/DD FSO-EH systems, we next differentiate between different EH procedures that can be associated with PAM, PPM and a novel modulation format. In particular, we focus on the energy-rate regions that can be achieved and on the associated impact on the system complexity. The features of the FSO-EH schemes are summarized in Table 1. These schemes are also depicted in Fig. 2 highlighting the impact of the transmission protocol on the DC component.

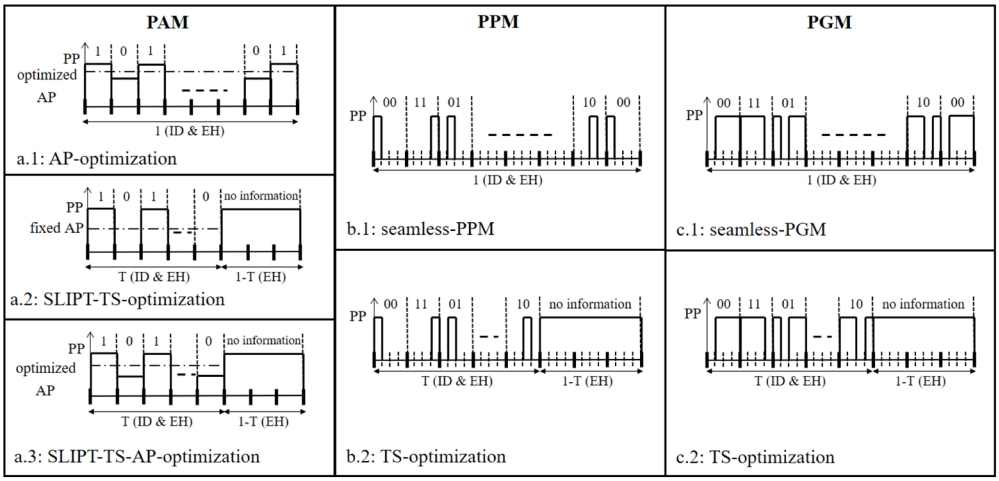

Fig. 2. The PAM, PPM and PGM FSO-EH schemes. The transmission time is normalized to 1 second and the parameter T stands for the TS ratio.

3.1. FSO-EH with PAM

As with the SLIPT-TS and SLIPT-TS-AP solutions, the proposed FSO-EH-PAM scheme is based on maximizing the harvested energy for a fixed target information rate denoted by R_{th}. In [12],

Table 1. Comparison between the different modulation-specific FSO-EH protocols

	PAM			PPM		PGM	
	AP-optimization	SLIPT-TS-optimization	SLIPT-TS-AP-optimization	Seamless	TS-optimization	Seamless	TS-optimization
Time Slotted	no	yes	yes	no	yes	no	yes
Slots	Slot-1: EH & ID	Slot-1: EH & ID Slot-2: EH	Slot-1: EH & ID Slot-2: EH	Slot-1: EH & ID	Slot-1: EH & ID Slot-2: EH	Slot-1: EH & ID	Slot-1: EH & ID Slot-2: EH
Required Optimization	optimize AP	optimize TS	optimize TS & AP	none	optimize TS	none	optimize TS
CSI Needed	yes	yes	yes	no	yes	no	yes

EH: energy harvesting, ID: information decoding, AP: average power, TS: time splitting.

Optics EXPRESS

the following capacity expression was used as a lower bound on the achievable rate:

$$R_1(P_{\text{av}}) = \log_2\left(1 + \frac{e}{2\pi}\left(\frac{\eta 10^{-\frac{L_{\text{atm}}}{10}} \min\{P_{\max} - P_{\text{av}}, P_{\text{av}} - P_{\min}\}}{\sigma}\right)^2\right), \tag{10}$$

where σ stands for the noise standard deviation.

We denote by T the fraction of time over which joint EH and ID occur while the fraction $1 - T$ is dedicated to pure EH in a time-splitting scheme. The SLIPT-TS protocol corresponds to carrying out the following optimization:

$$\max_{T}\left\{TE\left(\frac{P_{\min} + P_{\max}}{2}\right) + (1 - T)E(P_{\max})\right\} \tag{11}$$

$$\text{s.t. } TR_1\left(\frac{P_{\min} + P_{\max}}{2}\right) \geq R_{\text{th}}, \tag{12}$$

where, for this scheme, the AP satisfies (4) in the first time slot. In this case, in (10), $P_{\max} - P_{\text{av}} = P_{\text{av}} - P_{\min} = \frac{P_{\max} - P_{\min}}{2}$. The multiplication by T in (12) follows from the fact the ID occurs only in the first slot (with normalized duration T).

Similarly, the SLIPT-TS-AP optimization problem is given by:

$$\max_{T, P_{\text{av}}}\{TE(P_{\text{av}}) + (1 - T)E(P_{\max})\} \tag{13}$$

$$\text{s.t. } TR_1(P_{\text{av}}) \geq R_{\text{th}}, \tag{14}$$

where the AP value in the first slot (P_{av}) is optimized along with the ratio T.

It can be observed that the mathematical framework presented in [15,16] constitutes a more appropriate information-theoretic background for evaluating the information rate of the considered GtA FSO PAM-based communication system where the terrestrial FSO gateway is connected to the power grid. In [15], bounds on the capacity of the FSO intensity channel were derived under both a non-negativity constraint and a PP constraint. The capacity analysis presented in [15] was further developed and extended in [16]. In particular, the capacity expression provided in [15, eq. 11] will be used as an upper-bound on the information rate:

$$R_2(a) = \frac{1}{2}\log_2\left(1 + a(1 - a)\left(\frac{\eta 10^{-\frac{L_{\text{atm}}}{10}} P_{\max}}{\sigma}\right)^2\right), \tag{15}$$

where $a \triangleq \frac{P_{\text{av}}}{P_{\max}}$ stands for the average-to-peak power ratio (APPR) with $0 \leq a \leq 1$.

Based on [15, theor. 3] and [16, eq. 5], the capacity expression reported in (15) holds for all APPR values. Moreover, based on [16, eq. 5], for every APPR value below half, there exists an APPR value above half that achieves the same capacity. Therefore, since the amount of harvested energy increases with the AP (or, equivalently, with the APPR for a fixed PP), only values of a exceeding half will be considered. Therefore, without resorting to any time-splitting that turns out to be unnecessary in this case, the proposed EH-PAM scheme can be formulated as follows:

$$\max_{\frac{1}{2} \leq a \leq 1}\{E(aP_{\max})\} \tag{16}$$

$$\text{s.t. } R_2(a) \geq R_{\text{th}}, \tag{17}$$

where, for $\frac{1}{2} \leq a \leq 1$, (16) increases with a while (17) decreases with a.

Optics EXPRESS

Based on the above appraisal, the suggested AP-optimization-PAM scheme can be realized in a simple manner by solving the following quadratic equation for the values of a exceeding $\frac{1}{2}$:

$$a^2 - a + \frac{(2^{2R_{\text{th}}} - 1)\sigma^2}{\eta^2 10^{-\frac{L_{\text{atm}}}{5}} P_{\text{max}}^2} = 0, \tag{18}$$

which readily yields:

$$a = \frac{1}{2} + \sqrt{1 - \frac{4(2^{2R_{\text{th}}} - 1)\sigma^2}{\eta^2 10^{-\frac{L_{\text{atm}}}{5}} P_{\text{max}}^2}}, \tag{19}$$

for the values of R_{th} not exceeding $\frac{1}{2}\log_2\left(1 + \left(\frac{\eta 10^{-\frac{L_{\text{atm}}}{10}} P_{\text{max}}}{2\sigma}\right)^2\right)$.

Therefore, the proposed AP-optimization-PAM can be implemented in a simple manner, based on (18), without requiring any involved optimization techniques. The amount of harvested energy will be equal to $E(aP_{\text{max}})$ for the value of a derived in (18). Unlike the SLIPT solutions, the proposed scheme does not entail any time-splitting where information transmission and power transfer are concurrently realized over the entire transmission time. While the proposed AP-optimization-PAM and SLIPT-TS involve solving for only one variable (either a or T, respectively), the SLIPT-TS-AP corresponds to solving an optimization problem with two variables (AP over slot-1 and T) thus adding to the complexity of the receiver. Finally, all of the considered PAM solutions require acquiring the CSI in order to determine the optimal detection thresholds.

Finally, it is worth highlighting the following points pertaining to the comparison between the AP-optimization and SLIPT-TS-AP schemes. For the former scheme, increasing the value of a contributes to increasing the amount of harvested energy at the expense of reducing the achievable rate. In fact, when a increases, P_{av} approaches P_{max} incurring a reduction in the dynamic range where the difference between the power levels of the PAM symbols decreases. On the other hand, the SLIPT-TS-AP scheme can reduce the APPR value in the information-carrying part of the frame thus contributing to enhancing the decodability of the PAM symbols. However, dedicating a fraction of the time for mere energy harvesting will have a negative impact on the data rate where only a fraction T of the total time is dedicated for data communication. This is better illustrated in (14) where the achievable rate is multiplied by T. Therefore, for both schemes, the harvested energy can be compromised for the data rate and vice versa.

3.2. FSO-EH with PPM

For the sake of achieving the smallest BER and since the power consumption is not problematic at the transmitting ground unit, the laser is pulsed at PP in the "*on*" slot. This choice is also convenient for more efficient EH. Following from the attributes of the Q-PPM signal set, the associated FSO-EH can be implemented in two different ways thus allowing to achieve a tradeoff between EH-efficiency and complexity.

For the first scheme, EH is realized in a seamless manner without introducing any modification to the transmitted data stream of systems with no EH. In other words, over the entire transmission interval, each symbol duration comprises one "*on*" slot where the PP is transmitted and $Q-1$ "*off* " slots. At the receiver side, the DC component is separated from the received signal and fed to charge the battery of the UAV. This scheme is remarkably appealing because of its simplicity since its implementation does not entail any optimization or any CSI acquisition. The only modification to be introduced to the non-EH system in order to achieve seamless EH is the separation of the DC and AC components at the receiver by using an inductor and a capacitor in

Optics EXPRESS

parallel [12]. For this seamless scheme, the harvested energy is given by:

$$E\left(\frac{1}{Q}P_{\max}\right), \tag{20}$$

following from (5) and (8).

The second EH PPM scheme is based on TS and will be referred to as the TS-optimization-PPM scheme. In the first slot (with normalized duration T), PPM symbols are conveyed with one "*on*" slot and $Q-1$ "*off* " slots per symbol duration. Whereas in the second slot (with normalized duration $1-T$), the laser is pulsed at PP in all Q slots of each symbol duration for the sake of enhanced EH. In this case, the optimization problem can be solved in a straightforward manner where the fraction of time T can be simply obtained by dividing the target information rate by the information capacity:

$$T = \frac{R_{\text{th}}}{\log_2(Q) - \log_2\left(1 + (Q-1)\exp\left(-\frac{1}{2}\left(\frac{\eta 10^{-\frac{L_{\text{atm}}}{10}} P_{\max}}{\sigma}\right)^2\right)\right)}, \tag{21}$$

where the upper-bound on the constellation-constrained PPM capacity derived in [17] was used to approximate the information capacity.

Consequently, the amount of energy harvested by the TS-optimization-PPM scheme is given by:

$$TE\left(\frac{1}{Q}P_{\max}\right) + (1-T)E\left(P_{\max}\right), \tag{22}$$

for the value of T provided in (21).

As a conclusion, in addition to optimizing T, the TS-optimization-PPM scheme needs to acquire the CSI that is needed to determine the value of the information capacity.

3.3. FSO-EH with a novel modulation scheme

The absence of an AP constraint motivates the introduction of an EH-adapted pulse-based IM/DD modulation scheme that would increase the harvested energy at the UAV. This modulation format that is comparable to PPM will be referred to as pulse gap modulation (PGM). Unlike Q-PPM where the laser is pulsed in one slot (out of Q slots), the laser will be pulsed in $Q-1$ slots (out of the Q slots) for Q-PGM. In other words, the information will be modulated by the absence of a light pulse in contrast to PPM where the information is modulated by the presence of a light pulse. In this context, pulsing the laser more often will intensify the value of the DC component at the receiver thus enhancing the EH capabilities. In particular, the AP will be related to the PP by:

$$P_{\text{av}} = \frac{Q-1}{Q}P_{\max}, \tag{23}$$

where, compared to (5), the PGM energy will be harvested from a DC component that is $Q-1$ times bigger than the DC component attained by PPM.

As with PPM, seamless-PGM and TS-optimization-PGM constitute two viable options for PGM-based EH. In the seamless scenario, the harvested energy is given by:

$$E\left(\frac{Q-1}{Q}P_{\max}\right), \tag{24}$$

which shows improved levels of EH compared to seamless-PPM following from (20). Regarding the TS-optimization-PGM scheme, the optimization and CSI requirements are the same as with

Optics EXPRESS

TS-optimization-PPM since the information capacities of Q-PPM and Q-PGM are the same. In particular, the amount of harvested energy is given by:

$$TE\left(\frac{Q-1}{Q}P_{\max}\right)+(1-T)E\left(P_{\max}\right), \tag{25}$$

where T can be determined from (21).

4. Numerical results

The FSO transceiver parameters, the EH parameters and the weather-dependent parameters adopted for producing the simulation results are summarized in Table 2. The considered values constitute the typical values adopted in the literature [5,6,12]. In particular, we consider the cases of "clear air", "moderate rain" and "heavy rain" weather conditions. These weather conditions have a direct impact on the attenuation levels, rain losses and turbulence losses as highlighted in (6) and (7). As in [5], we consider an elevation angle of 45° where this angle affects the level of rain attenuation as per the link budget analysis presented in [5]. Finally, since the pointing losses are highly dependent on the implemented tracking system and since the design of such systems falls beyond the scope of this paper, we will assume constant pointing losses as in [5].

Table 2. The simulation parameters

FSO parameters			
Operating Wavelength (λ)			1550 nm
Receiver Responsivity (η)			0.5 A/W
Transmitted Power (P)			[10 200] mW
Noise standard deviation (σ)			10^{-7} A
Bandwidth (B)			250 MHz
Pointing losses (L_{poi})			2 dB
EH parameters			
Fill factor (f)			0.75
Dark saturation current (I_0)			10^{-9} A
Thermal voltage (V_t)			25 mV
Weather-dependent parameters			
Weather Condition	Attenuation coefficient (α)	Rain losses (L_{rain})	Refractive-index structure parameter (C_n^2)
Clear air	0.43 dB/km	0 dB/km	5×10^{-14} m$^{-2/3}$
Moderate rain (12.5 mm/hr)	5.8 dB/km	5.6 dB/km	5×10^{-15} m$^{-2/3}$
Heavy rain (25 mm/hr)	9.2 dB/km	10.2 dB/km	4×10^{-15} m$^{-2/3}$

Figure 3 shows the energy-rate regions of the FSO-EH schemes with PAM for a GtA link distance of 1 km under different weather conditions. The reported results clearly highlight on the significant amounts of energy that can be harvested especially under good weather conditions when the atmospheric losses are less pronounced. The tradeoff between the harvested energy and information rate can be easily observed from Fig. 3 where less energy is harvested at higher information rates. Regarding the comparison between the three PAM schemes, results in Fig. 3 show that the SLIPT-TS protocol results in the least harvested energy. It is worth highlighting that when comparing the AP-optimization method with the SLIPT solutions [12], the information rate is determined based on (15) rather than (10) for the sake of a fair comparison between the EH protocols.

The interesting conclusion that can be drawn from the results in Fig. 3 is related to the capability of the proposed AP-optimization scheme in achieving the same energy-rate tradeoff

Optics EXPRESS

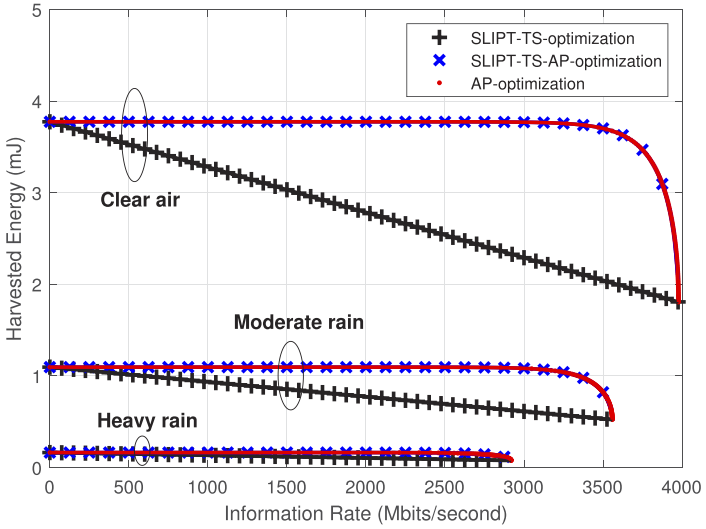

Fig. 3. FSO-EH with PAM for a link distance of 1 km under different weather conditions.

as the SLIPT-TS-AP scheme. In this context, the advantage of the former scheme resides in its simplicity since the associated optimization problem revolves around one variable rather than two variables as for the latter scheme. As previously highlighted, for the AP-optimization scheme, the optimal AP value can be readily obtained from (19) while, for the more sophisticated SLIPT-TS-AP scheme, more involved optimization techniques need to be implemented in to solve (13)–(14). Therefore, attempting to decrease the APPR in the information-carrying part of the frame by dedicating a fraction of this frame for EH (as in the SLIPT-TS-AP scheme) presents no particular advantage compared to transmitting at higher APPR values over the entire frame duration that is fully dedicated to information transmission (as in the AP-optimization scheme). In other words, the inherit tradeoff between energy harvesting and data rate entails that the transmission of a large number of symbols with a small dynamic range is equivalent to transmitting a smaller number of symbols with a higher dynamic range. As a conclusion, no particular advantage arises from coupling time splitting with average power optimization where the results reveal that the latter optimization is sufficient for achieving the same performance levels.

Figure 4 shows the energy-rate regions of the FSO-EH PPM and PGM protocols for a link distance of 1 km under "moderate rain" weather conditions. For Q-PPM, increasing the value of Q results in higher information rates since more bits are transmitted per PPM symbol. However, this advantage entails a reduction in the amount of harvested energy since the ratio of the "*on*" slots to the "*off* " slots will decrease thus diminishing the DC component at the receiver following from (20). These observations are well illustrated in Fig. 4 where signal sets with different cardinalities are compared. Figure 4 shows the advantages of the proposed PGM modulation scheme where, unlike PPM, increasing the cardinality of the signal set concurrently enhances the achievable information rate and the level of EH in coherence with (24). Even under the considered severe weather conditions that introduce significant losses, the EH-PGM protocols are capable of harvesting around 1 mJ of free energy from the information-carrying FSO signal with 8-PGM. The rationale behind the advised modulation scheme is also clear from Fig. 4 where PGM achieves enhanced EH levels compared to PPM. For example, for the seamless schemes, around eight times more energy can be harvested with 8-PGM than with 8-PPM.

Optics EXPRESS

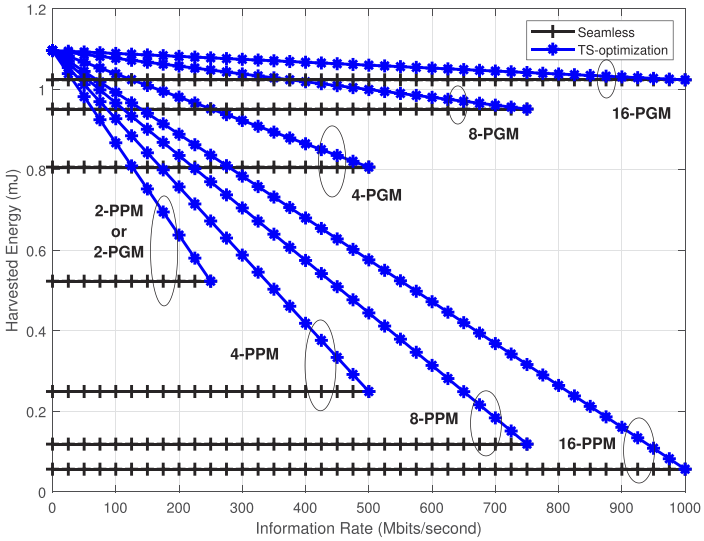

Fig. 4. FSO-EH with PPM and PGM for a link distance of 1 km under "moderate rain" weather conditions.

More importantly, Fig. 4 shows that, with both PPM and PGM, substantial amounts of energy can be harvested in a seamless manner without modifying the structure of the FSO transmitter. Evidently, the TS-optimization scheme results in larger amounts of harvested energy; however, this comes at the cost of an increased complexity. In this context, the gap between the seamless and TS-optimization protocols diminishes when the information rate is increased. This is justified by the fact that, when the rate increases, the portion of the transmission time dedicated to pure EH will decrease in order to meet the QoS requirement. Finally, the gap between the seamless-PGM and TS-optimization-PGM schemes is less pronounced than the gap between the seamless-PPM and TS-optimization-PPM schemes. In fact, for PGM, the amount of energy harvested in the joint EH-ID slot (slot-1) is significant thus inflicting a smaller duration on the EH slot (slot-2) and diminishing the impact of optimizing the TS ratio that will be very close to one. As shown in Fig. 4, the last observation is especially true for larger values of the signal set cardinality. For example, the amounts of energy harvested by the seamless and TS-optimization protocols are extremely close to each other in the case of 16-PGM.

5. Conclusion

For many state-of-the-art network architectures, relaying the information through UAVs constitutes an additional degree of freedom capable of leveraging the network's QoS and coverage. In the same spirit, this article proposed to leverage the battery lifetime of the flying platforms by harvesting some free energy from the information-carrying FSO signals. This energy complements the energy harvested from the terrestrial optical and RF WPT charging stations and contributes to enhancing the QoS of the end-to-end high speed links. Given the limited processing capabilities at the UAVs and since any involved processing and channel estimation at the UAV will drastically increase the power consumption, this work capitalised on the simplicity and practicality of the implemented EH strategies. We looked into different methodologies of FSO-EH from the power-grid-connected terrestrial FSO gateways depending on the constraints to be respected by the transmitted signal set. The adopted roadmap was culminated by the advisement of an EH-efficient modulation scheme. This open-loop scheme is capable of harvesting significant amounts of FSO signal energy while escaping from the tedious task of estimating the underlying

Optics EXPRESS

FSO channel and while avoiding all forms of parameter optimization. As a conclusion, high data rates and significant EH can be concurrently realized based on simple architectures by taking the specificities of the GtA FSO links into consideration.

References

1. M. A. Khalighi and M. Uysal, "Survey on free space optical communication: A communication theory perspective," IEEE Commun. Surveys Tuts. **16**(4), 2231–2258 (2014).
2. H. Baek and J. Lim, "Design of future UAV-relay tactical data link for reliable UAV control and situational awareness," IEEE Commun. Mag. **56**(10), 144–150 (2018).
3. P. Dinh, T. M. Nguyen, S. Sharafeddine, and C. Assi, "Joint Location and Beamforming Design for Cooperative UAVs with Limited Storage Capacity," IEEE Trans. Commun., Early Access (2019).
4. Y. Zeng, R. Zhang, and T. J. Lim, "Wireless communications with unmanned aerial vehicles: opportunities and challenges," IEEE Commun. Mag. **54**(5), 36–42 (2016).
5. M. Alzenad, M. Z. Shakir, H. Yanikomeroglu, and M.-S. Alouini, "FSO-based vertical backhaul/fronthaul framework for 5G+ wireless networks," IEEE Commun. Mag. **56**(1), 218–224 (2018).
6. W. Fawaz, C. Abou-Rjeily, and C. Assi, "UAV-aided cooperation for FSO communication systems," IEEE Commun. Mag. **56**(1), 70–75 (2018).
7. H. Wang, G. Ding, F. Gao, J. Chen, J. Wang, and L. Wang, "Power control in UAV-supported ultra dense networks: Communications, caching, and energy transfer," IEEE Commun. Mag. **56**(6), 28–34 (2018).
8. J. Ouyang, Y. Che, J. Xu, and K. Wu, "Throughput maximization for laser-powered UAV wireless communication systems," in *IEEE Int. Conf. on Commun. Workshops (ICC Workshops)*, 1–6 (2018).
9. B. Makki, T. Svensson, K. Buisman, J. Perez, and M.-S. Alouini, "Wireless energy and information transmission in FSO and RF-FSO links," IEEE Wireless Commun. Lett. **7**(1), 90–93 (2018).
10. L. R. Varshney, "Transporting information and energy simultaneously," in *IEEE Int. Symp. on Inf. Theory (ISIT)*, 1612–1616 (2008).
11. T. D. P. Perera, D. N. K. Jayakody, S. K. Sharma, S. Chatzinotas, and J. Li, "Simultaneous wireless information and power transfer (SWIPT): Recent advances and future challenges," IEEE Commun. Surveys Tuts. **20**(1), 264–302 (2018).
12. P. D. Diamantoulakis, G. K. Karagiannidis, and Z. Ding, "Simultaneous lightwave information and power transfer (SLIPT)," IEEE Trans. on Green Commun. and Networ. **2**(3), 764–773 (2018).
13. P. D. Diamantoulakis, K. N. Pappi, Z. Ma, X. Lei, P. C. Sofotasios, and G. K. Karagiannidis, "Airborne radio access networks with simultaneous lightwave information and power transfer (SLIPT)," in *IEEE Global Commun. Conf. (GLOBECOM)*, 1–6 (2018).
14. M. Safari and M. Uysal, "Relay-assisted free-space optical communication," IEEE Trans. Wireless Commun. **7**(12), 5441–5449 (2008).
15. A. Lapidoth, S. M. Moser, and M. A. Wigger, "On the capacity of free-space optical intensity channels," IEEE Trans. Inform. Theory **55**(10), 4449–4461 (2009).
16. R. Belli, J. Portugheis, and C. Runge, "On optimal non-equally spaced M-PAM in dimmable visible light communication," IEEE Photon. Technol. Lett. **29**(19), 1619–1622 (2017).
17. J. A. López-Salcedo and G. Vázquez, "Closed-form upper bounds for the constellation-constrained capacity of ultra-wideband communications," in *IEEE Int. Conf. on Acoustics, Speech and Signal Processing (ICASSP)* 3, 565–568 (2007).